

<https://doi.org/10.37501/soilsa/161944>

Simulation of soil water and nitrate transport in a wheat field under various nitrogen fertilizer rates and rainfed conditions using HYDRUS-1D

Abdelhakim Lahjouj^{1,2*}, Abdellah El Hmaidi², M'hamed Boufala², Karima Bouhafa¹

¹Laboratory of Water, Soil, and Plant, National Institute for Agricultural Research, Regional Center of Meknes, km 10, Haj Kaddour Road, P.O.Box 578 (VN), Meknes, Morocco

²Laboratory of Geo-engineering and Environment, Team "Water Science and Environmental Engineering", Department of Geology, Faculty of Sciences, Moulay Ismail University, P.O.Box 11202, Zitoune, Meknes, Morocco

* Abdelhakim Lahjouj, a.lahjouj@edu.umi.ac.ma, ORCID iD: orcid.org/0000-0001-9977-9058

Abstract

Received: 2022-06-19
Accepted: 2023-03-07
Published online: 2023-03-07
Associated editor: Z. Bakacsi

Keywords:

HYDRUS-1D
Nitrogen fertilization
Nitrate
Rainfed conditions
Soil water

In this study, we used HYDRUS-1D software to simulate soil water and nitrate ($\text{NO}_3\text{-N}$) transport in a rainfed wheat field under various nitrogen (N) fertilizer scenarios (0 to 126 kg ha⁻¹) in Morocco. We used inverse modeling to calibrate the input parameters involved in the simulation. The comparison between simulated and measured soil water (SWC) and $\text{NO}_3\text{-N}$ contents at different soil layers was carried out using the index of agreement (d), determination coefficient (R^2), $RMSE$, and MAE . By considering the soil profile (0–100 cm), acceptable SWC simulation accuracies were obtained for the calibration and validation steps ($d=0.88\text{--}0.94$, $R^2=0.67$ to 0.80, $RMSE=0.034\text{--}0.051$ cm³cm⁻³, and $MAE=0.024\text{--}0.038$ cm³cm⁻³), while $\text{NO}_3\text{-N}$ simulation was less accurate ($d=0.49\text{--}0.82$, $R^2=0.20\text{--}0.58$, $RMSE=0.015\text{--}0.068$ mg cm⁻³, and $MAE=0.012\text{--}0.046$ mg cm⁻³). In addition, the observed $\text{NO}_3\text{-N}$ contents showed a lack of significant differences in the root zone (20–100 cm) between N fertilizer rates ($p>0.05$), which was consistent with the lack of N fertilizer effects on simulated $\text{NO}_3\text{-N}$ leaching below the soil profile by HYDRUS-1D. The $\text{NO}_3\text{-N}$ leached amount accounted for 25 kg ha⁻¹ and was derived mainly from the initial soil N contents. The simulated N balance of the soil profile revealed that volatilization and denitrification were the major pathways of N fertilizer loss, accounting for about 3.8 and 51.7% of the N fertilizer rates, respectively. We suggest further studies to improve the simulation accuracies of HYDRUS-1D using sufficient calibration data from long-term wheat experiments to ensure effective N fertilization management in the study area.

1. Introduction

Several basins in Morocco, including the Saiss basin, are confronted with groundwater nitrate (NO_3^-) pollution (Fekkoul et al., 2012; Lahjouj et al., 2020a). Indeed, NO_3^- is considered the most abundant pollutant in groundwater (Masetti et al., 2007). NO_3^- pollution is often more serious where agricultural activities are intensive. Although Nitrogen (N) has a fundamental role in increasing crop yield, it may cause groundwater pollution. Several studies have reported that the overuse of N fertilizers has substantially increased NO_3^- concentrations in groundwater in several basins worldwide (Serio et al., 2018; Ogrinc et al., 2019). In addition, Pang et al. (1998) demonstrated the great effects of climatic conditions and N fertilizer rates on nitrate ($\text{NO}_3\text{-N}$) leaching risk. The overuse of N fertilizer may not significantly improve crop yield and N uptake due to several factors, including N accumulation and N losses through volatilization, denitrification, and leaching pathways (Liu et al., 2003; Wang et al., 2010; Zhang et al., 2015), however, it may even

reduce significantly crop yields, resulting in economic losses for farmers (Zotarelli et al., 2009; Badr et al., 2012). Therefore, researchers need to consider several factors to reduce N losses from soils and improve N fertilization management, including application timing, N rates, agro-climatic conditions, and physicochemical soil properties. Although the consumption of mineral N fertilizers in Morocco increases by an average of 5000 tons/year (MAFRDWF, 2019), very few studies have assessed the effects of N fertilizers on N accumulation and leaching at the field scale.

Soil water content (SWC) and $\text{NO}_3\text{-N}$ concentration measurements are often costly and difficult to carry out at the field scale. Therefore, calibrated and appropriate numerical models can be useful tools for assessing the impacts of N fertilizer, irrigation rates, and climatic conditions on SWC and $\text{NO}_3\text{-N}$ dynamics in different soil layers during the entire crop cycle. In addition, numerical simulation can also quantify N losses through different pathways (leaching, volatilization, and denitrification), improving N fertilization management at a local scale.

In recent years, several researchers have simulated soil water flow and N transport at the field scale (Hanson et al., 2006; Wallis et al., 2011; Marinov and Marinov, 2014), highlighting the importance of numerical models in N fertilization and irrigation management.

HYDRUS-1D and HYDRUS-2D/3D software packages (Šimůnek et al., 2008) are among the models that have been extensively used in the simulation of SWC and solute transport under various scenarios worldwide (Baram et al., 2016; Iqbal et al., 2020; Rezayati et al., 2020). These studies have demonstrated the ability of both models to effectively simulate water movement and to describe the complexity of solute transport and transformation processes, which are affected by the physical, chemical, and biological properties of the soil. Indeed, HYDRUS-1D and HYDRUS-2D/3D software packages simulate water and solutes transport using Richard's and advection/dispersion equations.

The application of numerical models on the simulation of $\text{NO}_3\text{-N}$ and SWC at the crop field scale in Morocco remains very limited. Most related studies have focused only on the simulation of SWC. Indeed, Bourziza et al. (2017) found that HYDRUS-2D can effectively simulate SWC under sub-surface drip irrigation in the southeastern part of Morocco. Although HYDRUS-2D/3D model can simulate water and solute movements more accurately than HYDRUS-1D, its discretization is more complex due to the consideration of two and three-dimensional domains. In addition, HYDRUS-2D/3D software requires more computational time compared to HYDRUS-1D, particularly when inverse modeling is used to optimize input parameters. Moreover, HYDRUS-1D is a public domain software, making it easily accessible.

Although HYDRUS-1D has been extensively used to simulate SWC water and N transport in soils, few studies have assessed its simulation accuracy under rainfed conditions. Moreover, to the best of our knowledge, the simulation of soil $\text{NO}_3\text{-N}$ content from mineral N fertilizers at the field scale has not been carried

out in Morocco. In this context, the main objectives of this study are 1) to assess the accuracy of the HYDRUS-1D software package for simulating SWC and $\text{NO}_3\text{-N}$ transport in the 0–100 cm soil profile under rainfed wheat and various N fertilizer scenarios; 2) to evaluate the impacts of N fertilizer rates and rainfed conditions on SWC and $\text{NO}_3\text{-N}$ distributions in the soil. The N balance for each N fertilizer scenario was also simulated and discussed in this study.

2. Materials and Methods

2.1. Field experiment

In this study, we conducted a field experiment with a wheat crop (*Triticum Aestivum L.*) from December 2018 to June 2019 under rainfed conditions at the station of the National Institute of Agricultural Research of Douyet, which is located in the Saiss basin ($34^{\circ}03'02.2''\text{N}$, $5^{\circ}05'08.4''\text{W}$, Altitude = 416 m) (Fig. 1). The basin is characterized by a semi-arid Mediterranean climate. The mean annual rainfall at the Douyet varies between 400 and 430 mm. The reason for not applying irrigation in this study is that the majority of the areas cultivated by wheat in the Saiss basin are under rainfed conditions.

Meteorological data of the studied period were recorded at a meteorological station located at the same field station. The rainfall amount during the growing season was about 172 mm, corresponding to 44% of the annual rainfall amount (Fig. 2). Indeed, most rainfall amounts occurred before sowing (234.2 mm). The daily mean air temperature was about 17.8°C , with minimum and maximum values of 6.3 and 32.5°C , respectively. Before wheat sowing, we collected soil samples from 5 consecutive soil layers (0–20, 20–40, 40–60, 60–80, and 80–100 cm). The results of the soil physicochemical characteristics are reported in Table 1, indicating predominantly silty clay loam soil.

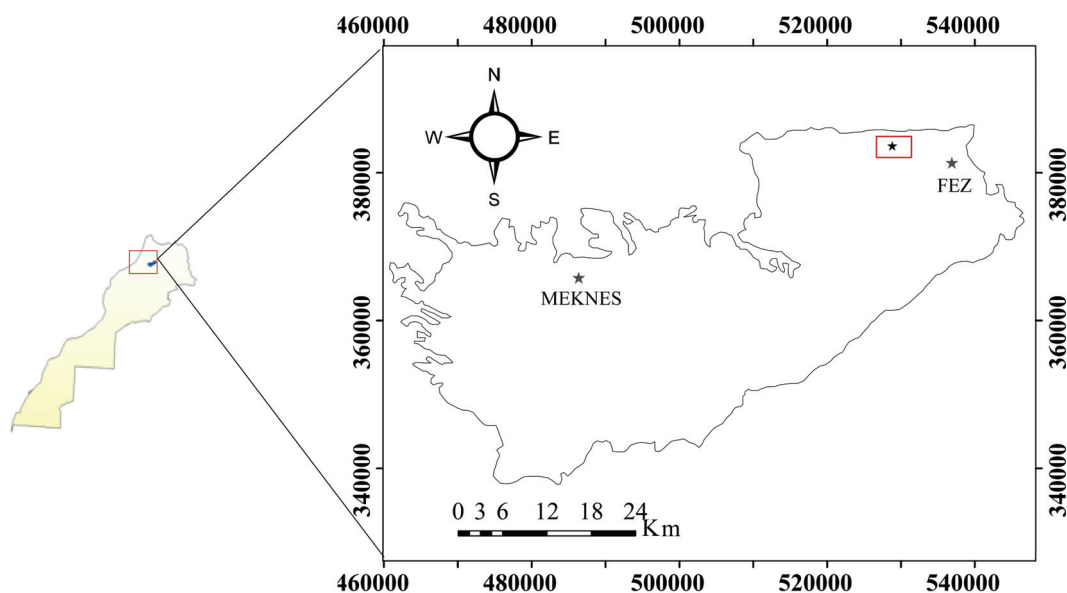


Fig. 1. Geographic location of the experimental field in the Saiss basin

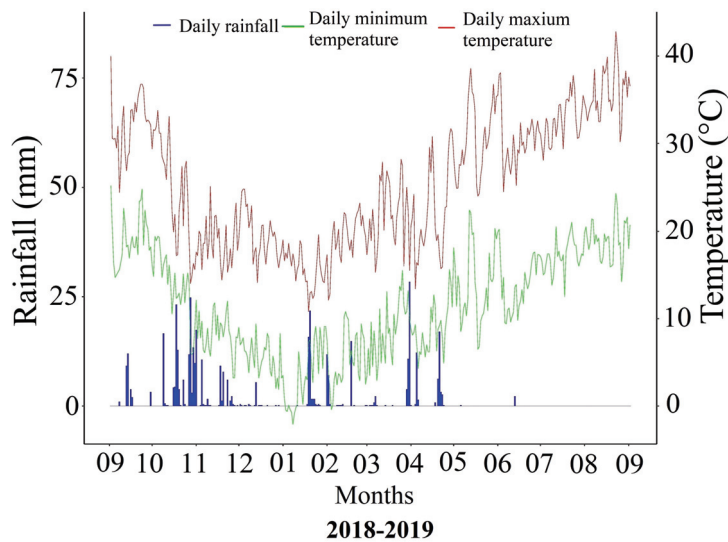


Fig. 2. Rainfall, minimum, and maximum temperature recorded at the experiment field over the 2018–2019 period

Table 1

Soil physicochemical characteristics of the experimental field

Soil depth cm	pH	NO ₃ mg kg ⁻¹	NH ₄ mg kg ⁻¹	SWC cm ³ cm ⁻³	Silt %	Clay %	Sand %	Bulk Density g cm ⁻³
0–20	7.40	26.68	30.32	0.300	58.83	28.44	13.00	1.55
20–40	7.46	34.35	45.64	0.346	58.10	29.80	12.35	1.59
40–60	7.47	50.91	6.38	0.360	63.44	25.52	11.53	1.65
60–80	7.76	25.52	2.07	0.330	60.28	28.00	11.81	1.70
80–100	7.81	25.06	–	0.320	56.20	31.04	11.92	1.69

2.2. Experimental field and soil sampling

The surface area of the field experiment cultivated with wheat was about 360 m². The wheat was sown on 26 December 2018 using the *Achtar* variety, which is widely cultivated by local farmers. In addition, we conducted the field experiment in a randomized complete block design with 3 replications and 6 plots/block (each was about 20 m²). Besides the control (N0), we have applied five N fertilizer rates at 21 (N1), 42 (N2), 63 (N3), 84 (N4), and 126 kg ha⁻¹ (N5), corresponding to 0, 25, 50, 75, 100, and 150% of the N fertilizer rates recommended for wheat crop in the region, respectively. In addition, each N rate was split into two applications, at sowing using ammonium sulfate (21%) ((NH₄)₂SO₄) and at the tillering stage (March) using ammonium nitrate (33.5%) (NH₄NO₃). No treatment with pesticides was applied during the experiment. In addition, we applied phosphorus and potassium at sowing at rates of 90 and 96 kg ha⁻¹ using triple superphosphate and potassium sulfate, respectively.

In this study, we monitored the SWC and NO₃-N contents at 42, 70, 96, 126, and 187 Days After Sowing (DAS). These dates were selected to reflect the SWC and NO₃-N contents at different wheat stages and following wheat harvest (187 DAS). On each date, we collected soil samples at the center of all plots (18) from five soil layers (0–20, 20–40, 40–60, 60–80, and 80–100 cm) using

a soil auger. We determined SWC using the gravimetric method by measuring the weights of the collected soil samples at the field, followed by oven-drying at the laboratory at 105°C until a constant weight was reached. In this study, we considered the volumetric SWC values by multiplying the measured gravimetric SWC values by bulk densities (ρ_s) of the soil layers (Table 1). Regarding soil samples intended for NO₃-N analysis, they were stored in plastic bags and analyzed using chromotropic acid after extraction with ammonium acetate (5:1 ratio). To determine the wheat yield, we sampled a 0.25 m² portion near the soil surface and at the center of each sub-plot at 150 DAS to determine the wheat yield components, namely the number of wheat ears (NE), number of grains per ear (NG/E), 1000 grains weight (g), and grain yield (kg ha⁻¹) (GY).

2.3. HYDRUS-1D software description

In this study, we applied the HYDRUS-1D software package to simulate SWC and NO₃-N movement using Richard's equation (Šimůnek et al., 2008). In addition, similar to many solutes' simulation studies using HYDRUS-1D, we simulated NO₃-N transport using the advection/dispersion equation. The equation governing the NO₃-N transport derived from NH₄-N nitrification is expressed as follows (Li et al., 2015):

$$\frac{\partial(\theta \cdot C_2)}{\partial t} = \frac{\partial \theta}{\partial z} \left[\theta \cdot D \left(\frac{\partial C_2}{\partial z} \right) \right] - \frac{\partial q \theta C_2}{\partial z} - \mu_w \theta C_2 + \mu'_w \theta C_1 - r_a \quad (1)$$

Where C_1 and C_2 denote $\text{NH}_4\text{-N}$ and $\text{NO}_3\text{-N}$ concentrations (mg cm^{-3}), respectively; D denotes the dispersion coefficient ($\text{cm}^2 \text{ day}^{-1}$); q denotes the volumetric flux density (cm day^{-1}); μ_w denotes the first-order rate (day^{-1}) for C_2 ; μ'_w denotes the first order providing concentration from C_1 ; r_a denotes the root N uptake ($\text{mg cm}^{-2} \text{ day}^{-1}$).

2.4. Initial boundary conditions and N fertilizer application

In this study, we simulated SWC and $\text{NO}_3\text{-N}$ transport for a total period of 187 days, using $1 \cdot e^{-008}$ and 1 as the minimum and maximum time steps, respectively. The first step in the simulation was to define the soil profile. Therefore, we discretized the entire soil profile (0–100 cm) into 100 nodes and classified it into 5 consecutive soil layers (0–20, 20–40, 40–60, 60–80, and 80–100 cm). During the simulation, no lateral water flow boundary was considered. The initial boundary condition was defined as atmospheric with surface layer (upper boundary condition) and free drainage (bottom boundary condition). In addition, we considered the initial observed SWC of each soil layer (Table 1) to define the initial SWC in the discretized soil profile in HYDRUS-1D software. Regarding $\text{NO}_3\text{-N}$ movement, we selected concentration boundary conditions and zero concentration gradient for the upper and lower boundary, respectively. Moreover, we specified the initial $\text{NO}_3\text{-N}$ concentrations in terms of mass volume⁻¹ of soil (mg cm^{-3}) in the discretized soil profile by converting the initial soil $\text{NO}_3\text{-N}$ and ammonium ($\text{NH}_4\text{-N}$) (mg kg^{-1}) to mg cm^{-3} . The first applied N rates on sowing were specified at the upper soil layer by considering that $(\text{NH}_4)_2\text{SO}_4$ was mixed with the first 5 cm soil layer. Regarding the second N rates (applied at the tillering stage using NH_4NO_3), we presented them at the soil surface by calculating the amount of each N element ($\text{NH}_4\text{-N}$ and $\text{NO}_3\text{-N}$) derived from NH_4NO_3 using molar mass.

2.5. N total and water root uptakes

The HYDRUS-1D software package uses the Feddes model to simulate root water uptake. According to Feddes et al. (1978), the equation used is described as follows:

$$S = \alpha(h) \times S_{max} \quad (2)$$

Where S denotes the root water uptake (cm day^{-1}); $\alpha(h)$ denotes the root water uptake (cm); S_{max} denotes the maximum root water uptake (cm day^{-1}).

In this study, we used the specific wheat root water uptake coefficients in the simulation, according to Wesseling et al. (1991). In addition, the maximum root depth of wheat was set at 100 cm (Fang et al., 2006). Whereas the total N uptake (NUP) was assumed as passive during the simulation for both $\text{NH}_4\text{-N}$ and $\text{NO}_3\text{-N}$. Therefore, the maximum daily N concentration of root uptake (C_{max}) was first obtained from the literature (2.7 to 6.5 $\text{kg ha}^{-1} \text{ day}^{-1}$) (Barraclough, 1986; Petersen, 2001; Malhi et al., 2006), then calibrated through several simulations.

Besides the observed daily rainfall, we used the Penman-Monteith method to estimate first the reference evapotranspiration (ET_0) and then determine the daily evapotranspiration (ETc) according to the following formula (Allen et al., 1998):

$$ETc = ET_0 \times K_c \quad (3)$$

Where K_c denotes the crop coefficient, including both soil evaporation and crop transpiration.

To differentiate between soil evaporation (K_e) and crop transpiration (K_{cb}), we adjusted the specific coefficients of wheat obtained from the FAO-56 database according to daily wind speed and daily minimum relative humidity data observed at the meteorological station.

The evapotranspiration amount was 327 mm, of which evaporation and transpiration amounts were 51.46 and 275.53 mm, respectively. In addition, the maximum evaporation and transpiration fluxes were observed during the initial and middle stages, respectively (Fig. 3).

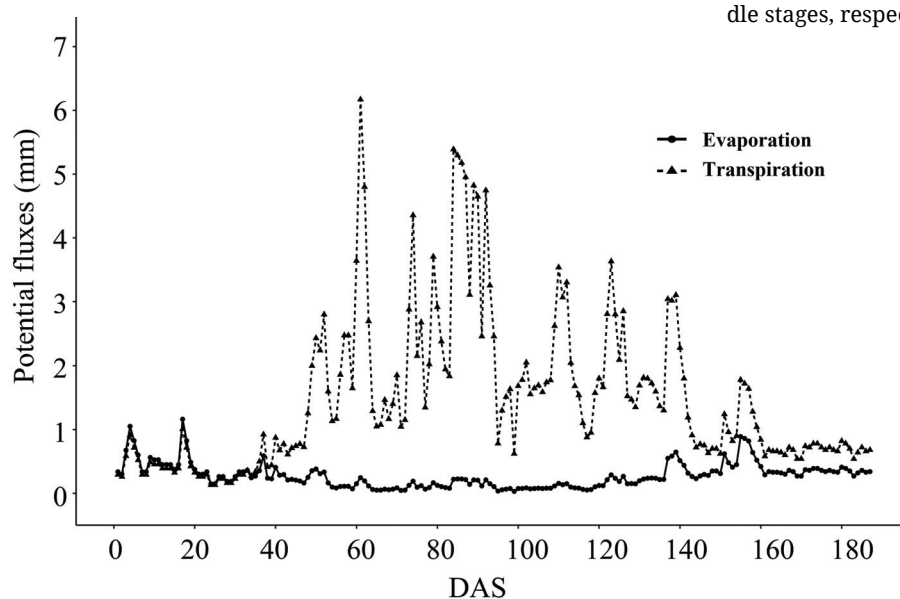


Fig. 3. Potential transpiration and soil evaporation rates

2.6. Calibration of input model parameters

In order to calibrate and validate HYDRUS-1D, we divided the observed data into two datasets. The objective of the calibration step was to optimize the input parameters governing the simulation of the SWC and $\text{NO}_3\text{-N}$ contents under varying N fertilizer ($(\text{NH}_4)_2\text{SO}_4$ and NH_4NO_3) applications. Therefore, we considered the wheat fertilization practices used in the field experiment (N applications at the sowing and tillering wheat stage) in the calibration step of HYDRUS-1D software to optimize the input parameters. In this study, we calibrated HYDRUS-1D using the observed mean SWC and $\text{NO}_3\text{-N}$ contents (calculated from the replications) during the entire wheat crop experiment (42, 70, 96, 126, and 187 DAS). However, we believe that the observed SWC and $\text{NO}_3\text{-N}$ data on these dates are insufficient to achieve an accurate and precise calibration of hydraulic and solute parameters of HYDRUS-1 for simulating precisely SWC and soil $\text{NO}_3\text{-N}$ contents during the entire season of wheat. In this study, we selected the first N fertilizer rate (N1) for the calibration step, while the remaining N fertilizer rates (N0, N2, N3, N4, and N5) were used for validation purposes. To estimate the hydraulic parameters (θ_s , θ_r , α , n , and K_s), we introduced the physical soil data (silt, clay, sand, and bulk density) to the Rosetta pedotransfer, then we calibrated the estimated values through several simulations using the Levenberg-Marquardt algorithm (Marquardt, 1963). According to Mualem (1976), the parameter l , representing the tortuosity effect, was set at 0.5.

The calibration of $\text{NO}_3\text{-N}$ simulation-related parameters is complicated due to the complex factors affecting N transport, such as soil pH, C: N ratio, soil aeration, and soil temperature. It was not possible to measure the parameters describing the $\text{NH}_4\text{-N}$ and $\text{NO}_3\text{-N}$ transformations and transport. Therefore, the minimum and maximum values of parameters related to N transport and transformation processes were obtained from the literature and optimized using inverse modeling. The molecular diffusion coefficients describing the distribution of $\text{NH}_4\text{-N}$ and $\text{NO}_3\text{-N}$ in free water were set at 1.52 and 1.64 $\text{cm}^2 \text{day}^{-1}$, respectively (Li et al., 2015), while the longitudinal dispersivity (D_L) was set at 20 cm (Phogat et al., 2014).

Unlike $\text{NO}_3\text{-N}$, which is considered to be present in free water, we assumed that $\text{NH}_4\text{-N}$ is adsorbed by soil particles according to the following formula (Kadyampakeni et al., 2018):

$$C_s = K_d \times C_w \quad (4)$$

Where C_s and C_w denote the $\text{NH}_4\text{-N}$ contents in the solid and liquid phases (mg cm^{-3}), respectively; K_d denotes the distribution coefficient of $\text{NH}_4\text{-N}$ ($\text{cm}^3 \text{mg}^{-1}$).

In this study, K_d was first set at 3.5 $\text{cm}^3 \text{g}^{-1}$ for all soil layers, then calibrated using inverse modeling (Ling and El-Kadi, 1998; Dash et al., 2014). In addition, we considered the nitrification process in the simulation since $(\text{NH}_4)_2\text{SO}_4$ and NH_4NO_3 were applied in the field experiment. The first-rate constant of the nitrification pathway was set at 0.2 day^{-1} (Hanson et al., 2006), then adjusted for each soil layer. Due to the fine texture and high-water retention capacity of the soil, we considered also the volatilization and denitrification pathways in the simulation as first-order decay reactions. In addition, we assumed the $\text{NH}_4\text{-N}$ volatilization and $\text{NO}_3\text{-N}$ denitrification pathways occur in the upper soil layer and entire root zone, respectively. Their first-order constant ranges were obtained from the literature (Li et al., 2015; Tan et al., 2015) and adjusted for each soil layer separately using the observed soil $\text{NO}_3\text{-N}$ contents to achieve minimal errors between the simulated and observed values. The N transformations considered in the simulation are described in Eq. (1). It should be noted that N transformations are temperature and water-dependent, which are often neglected in related studies on N transport simulation using HYDRUS-1D. The calibrated hydraulic and solutes parameters of different soil layers are reported in Table 2.

2.7. Statistical analysis and model evaluation

In this study, we analyzed the measured data using the one-way ANOVA test in R software V1.1.4 to determine whether the differences in SWC, $\text{NO}_3\text{-N}$ contents, and wheat yield components between N fertilizer rates were statistically significant (at $p < 0.05$). The requirement of data normality for the ANOVA test was checked using the test of Shapiro and Wilk (1965). In

Table 2
Optimized input parameters used in the simulation of SWC and $\text{NO}_3\text{-N}$ contents

Soil depth (cm)	θ_r ($\text{cm}^3 \text{cm}^{-3}$)	θ_s ($\text{cm}^3 \text{cm}^{-3}$)	α (1 cm^{-1})	n (-)	K_s (cm day^{-1})	l (-)	D_L (cm)	K_d ($\text{cm}^3 \text{g}^{-1}$)	r_{vol} (day^{-1})	r_{nit} (day^{-1})	r_{den} (day^{-1})
0–20	0.08	0.484	0.00567	1.9	1.4	0.5	20	4	0.001	0.2	0
20–40	0.082	0.454	0.0093	1.49	3.65	0.5	20	4		0.2	0.014
40–60	0.0874	0.464	0.0074	1.51	3.68	0.5	20	4		0.1	0.005
60–80	0.09	0.475	0.0084	1.45	2.47	0.5	20	4		0	0.013
80–100	0.09	0.462	0.0093	1.41	2.13	0.5	20	4		0	0

θ_r and θ_s denote the residual and saturated soil water contents, respectively; α and n are coefficient parameters of the soil water retention function; K_s and l denote the saturated hydraulic conductivity and tortuosity parameter, respectively; D_L and K_d denote the longitudinal dispersivity and adsorption isotherm coefficient, respectively; r_{vol} , r_{nit} and r_{den} are the first-order rate constants representing volatilization, nitrification, and denitrification, respectively.

addition, we used four statistical metrics to evaluate the simulation performance of HYDRUS-1D, namely the mean absolute error (*MAE*), root mean square error (*RMSE*), index of agreement (*d*) (Willmott 1995), and determination coefficient (R^2), according to the following equations:

$$d = 1 - \frac{\sum_{i=1}^N (Mi - Si)^2}{\sum_{i=1}^N (|Mi - M| + |Si - M|)^2} \quad (5)$$

$$R^2 = 1 - \frac{\sum_{i=1}^N (Si - Mi)^2}{\sum_{i=1}^N (Mi - M)^2} \quad (6)$$

$$RMSE = \sqrt{\frac{\sum_{i=1}^N (Si - Mi)^2}{N}} \quad (7)$$

$$MAE = \frac{\sum_{i=1}^N |Si - Mi|}{N} \quad (8)$$

Where *Mi* and *Si* denote the measured and simulated values, respectively; *N* denotes the number of measurements; *M* denotes the mean measured value.

The *RMSE* and *MAE* values close to 0 indicate that the simulated are close to the measured values, while *d* and R^2 vary between 0 and 1, corresponding to invalid and perfect simulation results, respectively.

3. Results and discussion

3.1. Measured SWC and NO₃-N

The one-way ANOVA results showed the lack of significant effects of N fertilizer rates on SWC in all soil layers ($p > 0.05$) (Table 3). The mean SWC varied from 0.231 ± 0.093 to 0.307 ± 0.087 $\text{cm}^3 \text{cm}^{-3}$. The highest and lowest SWC values were observed at the bottom and upper soil layers, respectively. Regarding NO₃-N content, the highest concentrations were observed at the upper soil layer and tended to decrease with soil depth. Compared to the control plot (N0), N fertilizer rates above 42 kg ha^{-1} increased significantly NO₃-N concentrations at the 0–20 cm soil layer ($p < 0.05$), from 39.4 ± 15.2 mg kg^{-1} to 116.43 ± 54.1 mg kg^{-1} (Table 3), while no significant differences were observed at the remaining soil layers ($p > 0.05$), suggesting an accumulation of N fertilizer at the upper soil layer.

3.2. Model calibration and validation results

The simulation accuracy results of the calibration and validation steps of SWC and NO₃-N at different soil layers are reported in Table 4. According to the obtained results, the 20–40 soil layer showed the lowest *d* and R^2 values between the simulated and observed SWC in the calibration step ($d = 0.42$; $R^2 = 0.11$). Whereas in the remaining soil layers, the *d* and R^2 values ranged from 0.94 to 0.97 and 0.84 to 0.99, respectively, suggesting reasonable simulation results of the calibration step. In addition, the *RMSE* and *MAE* values were lower than $0.07 \text{ cm}^3 \text{cm}^{-3}$, which is consistent with the findings of Kandelous and Šimůnek (2010) and Wang et al. (2014) (0.01 – $0.06 \text{ cm}^3 \text{cm}^{-3}$). Due

Table 3

Mean SWC ($\text{cm}^3 \text{cm}^{-3}$) and NO₃-N (mg kg^{-1}) values observed at different N fertilizer rates

Treatment kg ha^{-1}	Parameters	Sampling depth (cm)				
		0–20	20–40	40–60	60–80	80–100
N0	SWC	0.243±0.112a	0.231±0.093a	0.273±0.109a	0.290±0.075a	0.287±0.072a
N1		0.266±0.074a	0.256±0.063a	0.278±0.08a	0.300±0.084a	0.305±0.073a
N2		0.246±0.102a	0.278±0.086a	0.254±0.063a	0.294±0.089a	0.284±0.064a
N3		0.264±0.111a	0.256±0.074a	0.260±0.073a	0.287±0.079a	0.292±0.070a
N4		0.260 ± 0.101a	0.238±0.07a	0.287±0.074a	0.300±0.075a	0.299±0.073a
N5		0.258 ± 0.106a	0.264±0.066a	0.268±0.063a	0.282±0.071a	0.307±0.087a
N0	NO ₃ -N	39.4±15.2b	33.66±10.3a	29.1±12.4a	24.47±11.6a	23±10.25a
N1		42.5±22.3b	34.27±19.55a	29.9±14.4a	22.1±11.9a	25.5±14.45a
N2		54.7±31.5b	33.62±13.6a	31.77±12.15a	28.5±18.5a	25±12.58a
N3		65±23.1ab	44.30±23.8a	40.6±14.16a	29.7± 16.3a	24.56±12.77a
N4		75.45±17.42ab	41.2±15.8a	51.07±24.7a	36.4±19.4a	37.7±16.3a
N5		116.43±54.1a	66.7±29.6a	37.44±15.45a	41±17.5a	36.62±19a

Means from 3 blocks with the same letter within each soil layer are not significantly different between N fertilizer rates at $p < 0.05$. N0, N1, N2, N3, N4, and N5 correspond to 0, 21, 42, 63, 84, and 126 kg N ha^{-1} , respectively.

Table 4Model simulation accuracies of SWC and NO₃-N at different soil layers for the calibration (N1) and validation (N0, N2, N3, N4, and N5)

Soil depth (cm)	SWC					NO ₃ -N			
	N treatment	d	R ²	RMSE cm ³ cm ⁻³	MAE cm ³ cm ⁻³	d	R ²	RMSE mg cm ⁻³	MAE mg cm ⁻³
0-20	N1	0.97	0.91*	0.022	0.020	0.71	0.65	0.027	0.02
20-40		0.42	0.11	0.065	0.04	0.73	0.49	0.021	0.017
40-60		0.94	0.84	0.035	0.024	0.80	0.50	0.015	0.012
60-80		0.97	0.90	0.025	0.021	0.82	0.60	0.011	0.009
80-100		0.97	0.99***	0.018	0.017	0.51	0.32	0.019	0.013
All depth		0.92	0.74***	0.037	0.024	0.72	0.50***	0.019	0.014
0-20	N0	0.81	0.53	0.072	0.06	0.73	0.52	0.024	0.019
20-40		0.84	0.57	0.057	0.046	0.88	0.81*	0.013	0.011
40-60		0.91	0.74	0.051	0.042	0.77	0.44	0.017	0.016
60-80		0.95	0.82*	0.027	0.023	0.92	0.80*	0.010	0.009
80-100		0.91	0.78*	0.032	0.022	0.90	0.92***	0.009	0.007
All depth		0.88	0.67***	0.051	0.038	0.82	0.58***	0.015	0.012
0-20	N2	0.96	0.99***	0.032	0.025	0.57	0.15	0.051	0.042
20-40		0.78	0.36	0.059	0.040	0.79	0.46	0.014	0.012
40-60		0.92	0.84*	0.033	0.030	0.85	0.55	0.012	0.01
60-80		0.97	0.92**	0.022	0.020	0.74	0.84	0.021	0.018
80-100		0.97	0.95**	0.017	0.014	0.59	0.50	0.015	0.011
All depth		0.93	0.77***	0.035	0.026	0.65	0.36**	0.027	0.019
0-20	N3	0.95	0.94**	0.037	0.03	0.54	0.17	0.053	0.044
20-40		0.76	0.30	0.064	0.042	0.64	0.44	0.032	0.022
40-60		0.96	0.88	0.028	0.021	0.52	0.11	0.027	0.020
60-80		0.99	0.97**	0.015	0.013	0.66	0.45	0.022	0.014
80-100		0.96	0.95**	0.022	0.018	0.70	0.80*	0.014	0.010
All depth		0.93	0.78***	0.037	0.025	0.58	0.46***	0.032	0.022
0-20	N4	0.95	0.90	0.036	0.029	0.34	0.09	0.065	0.057
20-40		0.81	0.44	0.052	0.038	0.56	0.06	0.025	0.021
40-60		0.94	0.89*	0.035	0.028	0.50	0.01	0.048	0.034
60-80		0.98	0.96**	0.015	0.013	0.68	0.93**	0.031	0.025
80-100		0.96	0.94**	0.020	0.018	0.60	0.89	0.032	0.026
All depth		0.94	0.80***	0.034	0.025	0.49	0.20*	0.043	0.033
0-20	N5	0.95	0.90	0.039	0.034	0.45	0.35	0.13	0.11
20-40		0.74	0.35	0.063	0.046	0.58	0.80*	0.055	0.047
40-60		0.90	0.73	0.042	0.034	0.86	0.70	0.014	0.012
60-80		0.99	0.98**	0.012	0.012	0.62	0.78*	0.036	0.031
80-100		0.92	0.88	0.034	0.026	0.59	0.77*	0.033	0.024
All depth		0.90	0.70***	0.041	0.030	0.50	0.54***	0.068	0.046

N0, N2, N3, N4, and N5 correspond to 0, 42, 63, 84, and 126 kgN ha⁻¹, respectively; *, **, and *** denote significant determination coefficients at p<0.05, 0.01, and 0.001, respectively; SWC denotes soil water content; d, R², RMSE, and MAE denote the index of agreement, determination coefficient, root mean square error, and mean absolute error, respectively.

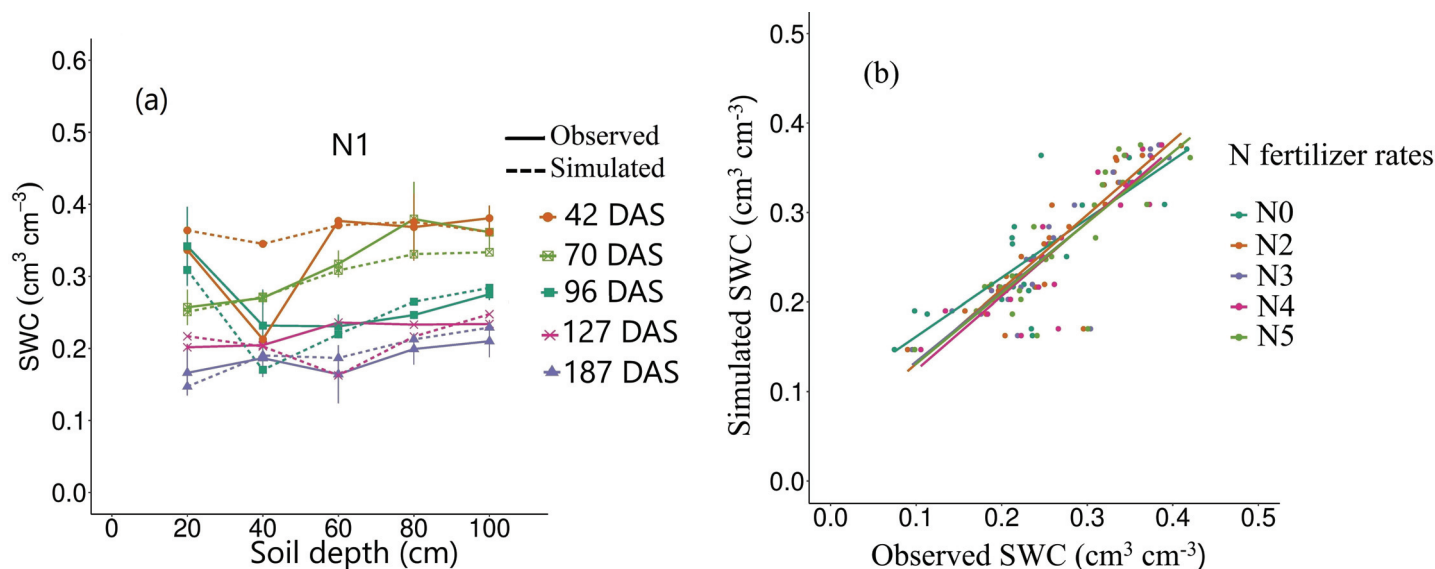


Fig. 4. Simulated and observed SWC in the calibration (a) and validation (b) NO, N1, N2, N3, N4, and N5 correspond to 0, 21, 42, 63, 84, and 126 kgN ha⁻¹, respectively

to the insufficient observed SWC data over the entire wheat season, the simulated and observed values were plotted versus soil depth instead of DAS. The simulated SWC tendency was consistent with the measured SWC (Fig. 4a). The simulated SWC was relatively constant across the soil profile at 42 DAS. However, the simulated and measured SWC in the root zone decreased considerably from 96 DAS due to the increase in wheat water requirements and the decrease in rainfall amounts from 70 DAS.

During the experiment, no irrigation was applied. Therefore, the simulated SWC values obtained in the calibration were the same as those obtained in the validation step in all N fertilizer scenarios. Moreover, the observed SWC showed a lack of significant differences between N rates ($p > 0.05$) (Table 3). Therefore, we used the same simulated SWC values to assess the simulation accuracies of the validation results. Visually, linear trends were observed between the observed and simulated values (Fig. 4b). The d and R^2 values of soil layers in the validation step ranged from 0.74 to 0.99 and 0.30 to 0.99, respectively (Table 4). By considering the entire soil profile, the d and R^2 values ranged from 0.88 to 0.94 and 0.67 to 0.80, respectively, while the $RMSE$ and MAE values were lower than 0.06 cm³ cm⁻³, indicating an acceptable simulation performance. Dash et al. (2014) and Narjary et al. (2020) showed comparable simulation accuracies of SWC using HYDRUS-1D in the validation step. Therefore, the optimized hydraulic parameters (Table 2) used in this study resulted in minimal errors between the simulated and observed SWC values at 42, 70, 96, 126, and 187 DAS. Regarding NO₃-N, the simulation accuracy during the calibration step was less satisfactory than that of SWC. The d , R^2 , $RMSE$, and MAE value ranges were 0.51–0.82, 0.32–0.65, 0.011–0.027 mg cm⁻³, and 0.009–0.017 mg cm⁻³ respectively. The same finding was observed in the validation step using the remaining N rates (Table 4 and Fig. 5). By considering the entire soil profile, the d , R^2 , $RMSE$, and MAE

value ranges in the validation step were 0.49–0.82, 0.20–0.58, 0.015–0.068 mg cm⁻³, and 0.012–0.046 mg cm⁻³, respectively (Table 4). These calibration and validation results are consistent with those reported in previous studies, showing lower accuracy of HYDRUS-1D software in simulating soil NO₃-N contents compared to SWC (Ebrahimian et al. 2012; Mokari et al. 2019). Nevertheless, HYDRUS-1D simulated well the effects of N fertilizer rates in this study at 42 and 96 DAS following N fertilizer applications. The lowest and highest simulated values were observed at N0 and N5, respectively. Moreover, the impacts of N rates on residual NO₃-N contents were also reasonably simulated. The simulated residual NO₃-N contents at 187 DAS in the entire soil profile increased from 0.034 to 0.164 mg cm⁻³ at N0 and N5, respectively, corresponding to 0.001 mg cm⁻³ kgN⁻¹. However, the simulated NO₃-N contents were slightly lower than the measured NO₃-N contents (Fig. 5). Besides the insufficient data used for calibrating HYDRUS-1D software, this underestimation might be due to the ignorance of other factors affecting NO₃-N transport in the simulation (e.g., organic matter mineralization, N immobilization, soil temperature, and C:N ratio) (Tan et al., 2015; Chen et al., 2022). In addition, the $RMSE$ and MAE values increased with increasing N rates, particularly at the upper soil layer, resulting in higher simulation errors than those at deeper soil layers due to the less change in NO₃-N at deeper soil layers between N rates, which is consistent with the results of Ramos et al. (2012). Moreover, the consideration of several solute parameters in the inverse solution to calibrate HYDRUS-1D in this study might contribute to the increase in the $RMSE$ and MAE values. For example, the optimized solute parameters showed constant D_L values across the entire soil profile, even though this solute parameter is affected by several factors, including soil texture, soil heterogeneity, and water flow rates (Gelhar et al. 1992; Hanson et al. 2006; Phogat et al. 2014; Azad et al. 2019).

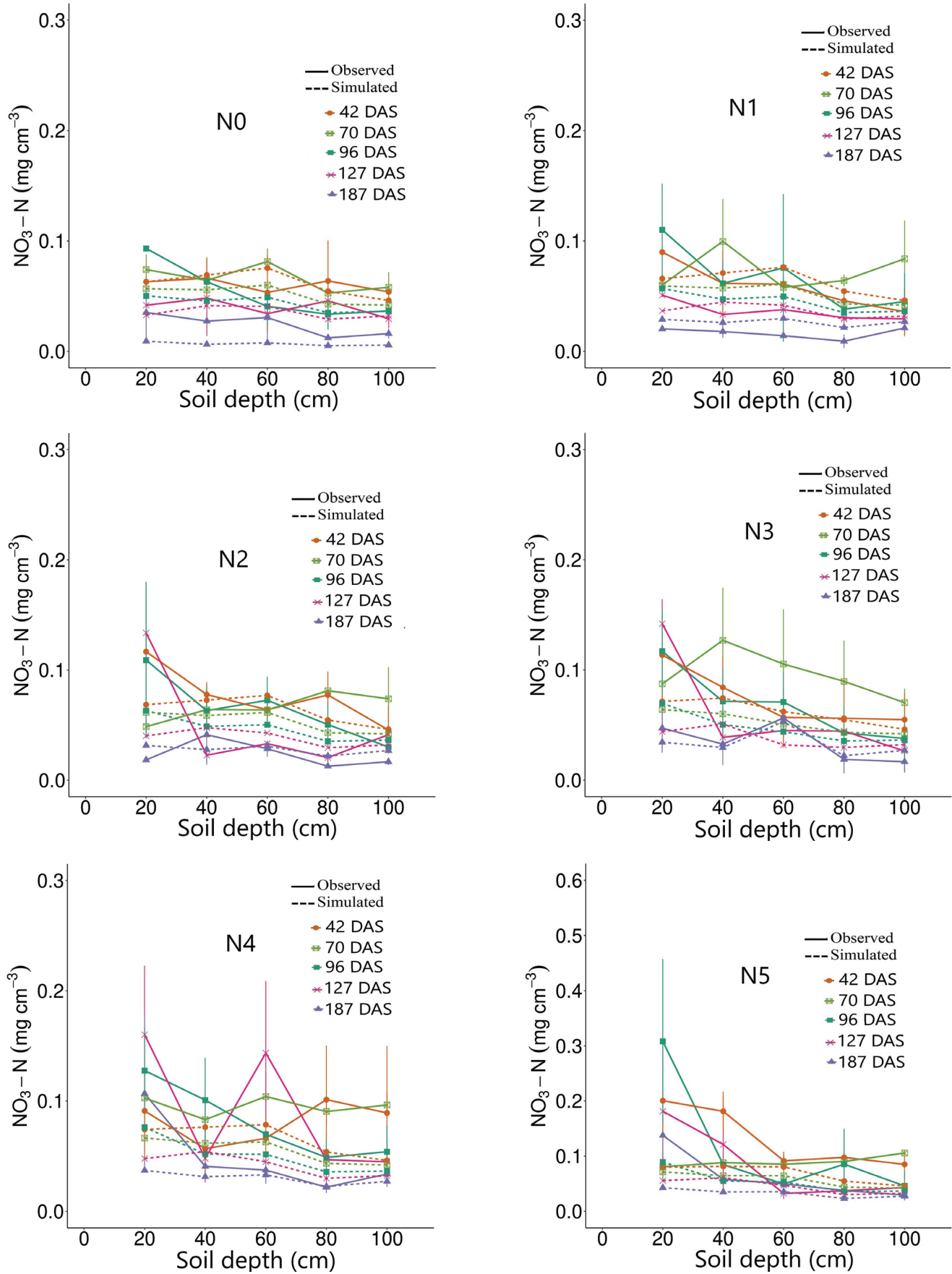


Fig. 5. Simulated and observed $\text{NO}_3\text{-N}$ in the calibration (N1) and validation (N0, N2, N3, N4, and, N5). N0, N1, N2, N3, N4, and N5 correspond to 0, 21, 42, 63, 84, and 126 kgN ha^{-1} , respectively

3.3. Water-deep percolation and $\text{NO}_3\text{-N}$ leaching

The mean daily rate of percolated water (below the 0–100 cm profile) was about $0.124 \text{ mm day}^{-1}$ (Fig. 6a). The simulated amount of percolated water over the wheat season was 19.8 mm, corresponding to 11% of the total rainfall recorded over the field experiment. Most of the percolated water amount was observed in the initial wheat stage, which is due to the low water requirement for wheat and the high SWC (Liao et al., 2008). Moreover, water infiltration below the upper soil layer was substantial during this stage (Fig. 7), showing an average water infiltration value of 4 mm day^{-1} . However, although the highest water infiltration rate at the upper soil layer was observed at 93 DAS, the percolated amount of water was negligible, showing a continuous decrease from 51 to 100 DAS, corresponding to the middle stage of wheat (Fig. 6a). This finding is due to the insufficient rainfall amount, as well as the gradual increase in temperature and wheat water requirement, decreasing the average observed SWC in the 20–100 cm soil layer from 0.360 to $0.225 \text{ cm}^3 \text{ cm}^{-3}$ at 42 and 127 DAS, respectively. Moreover, the average potential transpiration flux during the middle stage of wheat was 2.5 mm day^{-1} , with a maximum value of 6.17 mm day^{-1} (Fig. 3), decreasing the percolated

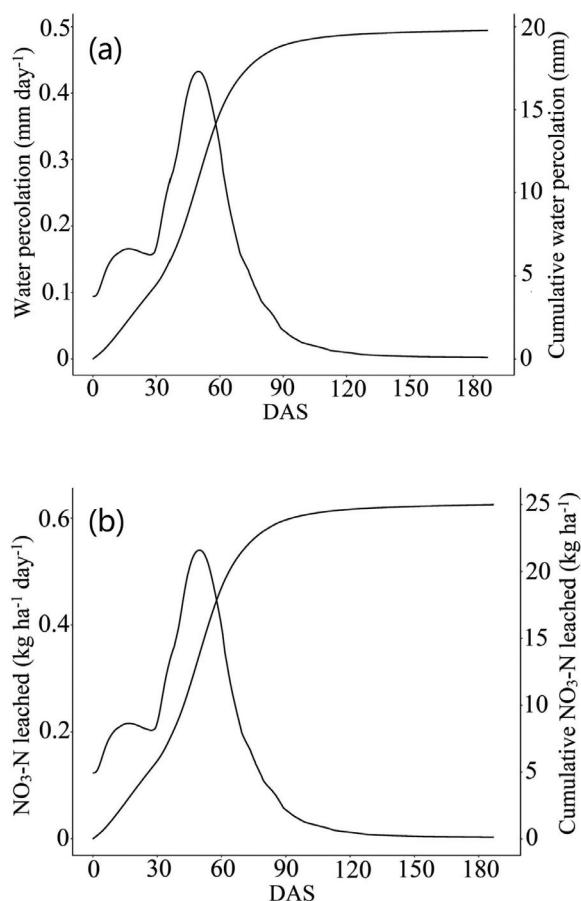


Fig. 6. Simulated daily and cumulative water percolation flux (a) and daily and cumulative $\text{NO}_3\text{-N}$ leaching (b) below the 0–100 cm soil profile in all N scenarios

water amount. The simulated root water uptake in this study accounted for 251 mm Ha^{-1} , which is slightly lower than the estimated transpiration amount (275.53 mm). These findings suggest that slight water stress might occur during the middle stage of wheat, which is consistent with Zhou et al. (2012).

$\text{NH}_4\text{-N}$ transport was limited in the soil profile since $\text{NH}_4\text{-N}$ tends to adsorb to the solid phase of the soil (Azad et al., 2019). The simulation results showed a negligible leached $\text{NH}_4\text{-N}$ amount. In contrast, $\text{NO}_3\text{-N}$ was the main N form leached below the soil profile and was correlated with the percolated water (Fig. 6b). The highest daily $\text{NO}_3\text{-N}$ leaching rates were observed in the initial wheat stage. The mean daily $\text{NO}_3\text{-N}$ leaching rate was about $0.15 \text{ kg ha}^{-1} \text{ day}^{-1}$, with a maximum value of $0.54 \text{ kg ha}^{-1} \text{ day}^{-1}$ observed at 49 DAS. However, the simulation results showed a lack of differences in the $\text{NO}_3\text{-N}$ leaching amounts between the control and N fertilizer rates. The amount of $\text{NO}_3\text{-N}$ leached accounted for 25 kg ha^{-1} in all fertilization scenarios, indicating that the initial soil $\text{NO}_3\text{-N}$ and $\text{NH}_4\text{-N}$ contents were the main sources of $\text{NO}_3\text{-N}$ leaching. This finding is consistent with the significant ($p < 0.05$) and insignificant ($P > 0.5$) accumulations of $\text{NO}_3\text{-N}$ contents in the upper soil layer (0–20 cm) and root zone (20–100 cm), respectively (Table 3). Indeed, $\text{NO}_3\text{-N}$ accumulation might be due to the low hydraulic conductivity and high-water retention capacity of the soil in the experimental station in Douyet. Moreover, the statistically significant $\text{NO}_3\text{-N}$ accumulation in the upper soil layer (Table 3) is consistent with the specific groundwater vulnerability to $\text{NO}_3\text{-}$ in the Saiss basin reported by Lahjouj et al. (2020b), showing a low vulnerability class to $\text{NO}_3\text{-}$ in the Douyet's surface area. However, further long-term investigations are required to determine the impacts of rainfall amount and supplemental irrigation on percolated water and leached $\text{NO}_3\text{-N}$ amounts.

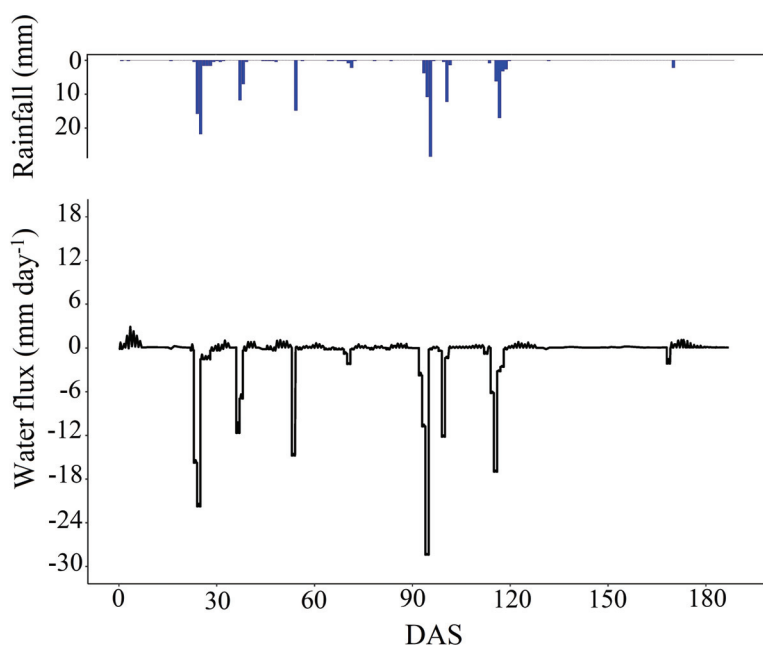


Fig. 7. Simulation of the actual surface flux in the upper soil layer. Negative and positive values indicate infiltration and evaporation, respectively

3.4. Measured wheat yield and nitrogen balance

The measured wheat yield components, namely NE, NG/ear, 1000 grains weight, and GY, were not significantly different between N fertilizer rates ($p>0.05$) (Table 5). Bendidi et al. (2013) showed similar results at the same field station and under rainfed and limited precipitation conditions. The grain yield varied between 806.5 and 1035.6 kg ha⁻¹. The irregular, insufficient rainfall amount, and gradual increase in wheat water requirements, particularly during the middle wheat stage (Fig. 2), were probably the main factors resulting in low wheat yield and insignificant effects ($p>0.05$) of N fertilizer rates on wheat yield due to their effects on the root water uptake and NUP. This result is consistent with the considerable decrease in the simulated percolation water and observed SWC at 70, 96, and 127 DAS in the root zone (20–100 cm), as mentioned above. The cumulative N

balance of the soil profile is reported in Table 6. Besides NUP and NO₃-N leaching, we considered the volatilization and denitrification processes in the simulated N balance. The simulated NUP values did not show a difference between N fertilizer rates. The total NUP amount was 40.7 kg ha⁻¹ in the control and N fertilizers scenarios (Fig. 8), indicating that NUP was derived from the initial soil N content. This finding is, indeed, consistent with the lack of significant effects of N fertilizer rates on the measured wheat yield components ($p>0.05$) (Table 5), as previous studies have pointed out a significant positive relationship between NUP and wheat yield (Yang et al., 2018; Wallace et al., 2020). Besides the decrease in rainfall amount, the lack of significant differences in the simulated NUP between N fertilizer rates might be due to two other reasons: 1) N fertilizer applied resulted in an obvious accumulation of NO₃-N contents in the upper soil layer (Fig. 5) due to the low soil hydraulic conductivity, high soil com-

Table 5
Effects of N fertilizer rates on the measured wheat yield components

N rate kg ha ⁻¹	NE m ²	NG ears	Weight of 1000 grains g	GY kg ha ⁻¹
N0	153a	22a	34.85a	806.5a
N1	180a	21a	34.23a	807a
N2	221a	18a	33.72a	1035.6a
N3	144a	19a	34.43a	793.51a
N4	213a	19a	32.02a	982.38a
N5	165a	19a	32.23a	863.44a

Means with the same letter are not significantly different among N fertilizer rates at $p<0.05$; NE, NG, and GY denote the number of ears, number of grains/Ear, and Grain yield, respectively; N0, N1, N2, N3, N4, and N5 correspond to 0, 21, 42, 63, 84, and 126 kgN ha⁻¹, respectively.

Table 6
Simulated N balance of the 0–100 cm soil profile

Balance components	N0	N1	N2	N3	N4	N5
Initial NH ₄ -N (kg ha ⁻¹)	269					
Initial NO ₃ -N (kg ha ⁻¹)	534					
NH ₄ -N added (kg ha ⁻¹)	0	12.86	25.72	38.6	51.47	77.23
NO ₃ -N added (kg ha ⁻¹)	0	8.14	16.28	24.4	32.53	48.77
NO ₃ -N uptake (%N)	5.1	0	0	0	0	0
Volatilization (%N)	1.9	4	3.4	3.8	3.8	3.8
Volatilization (% NH ₄ -N)	5.6	6.5	5.6	6.3	6.3	6.2
NO ₃ -N Leaching (%N)	3.1	0	0	0	0	0
Denitrification rate (%N)	58	52.3	51.2	51.5	51.6	52.1
NH ₄ -N residual (%N)	0.82	0	0	0	0	0
NO ₃ -N residual (%N)	31.6	59	57.2	57.9	57.9	58.7
N balance error (%)	-0.53	-15.3	-11.7	-13.3	-13.3	-14.6

N0, N1, N2, N3, N4, and N5 correspond to 0, 21, 42, 63, 84, and 126 kgN ha⁻¹, respectively

Initial N contents and N applied were considered as 100% for the control (N0) and remaining rates (N1, N2, N3, N4, and N5), respectively.

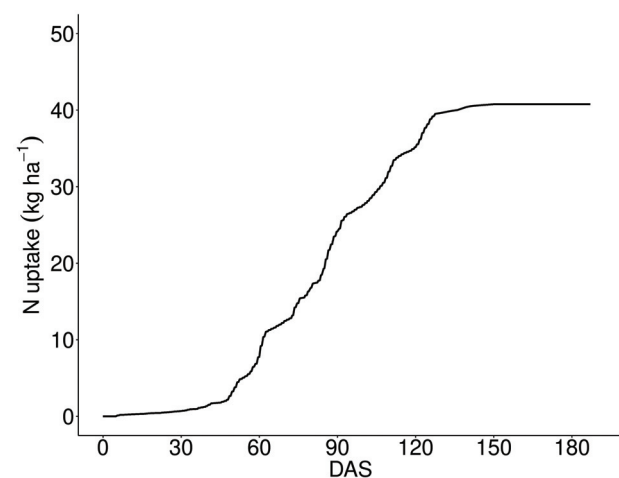


Fig. 8. Cumulative NUP (kg ha⁻¹) in all N scenarios

paction, and considerable decrease in rainfall amount, affecting $\text{NO}_3\text{-N}$ transport towards the root zone. As mentioned above, the one-way ANOVA results showed a lack of significant differences in $\text{NO}_3\text{-N}$ contents observed within the 20–100 cm soil layer (root zone) between N fertilizer rates ($p > 0.05$), decreasing the positive effects of N fertilizer rates on NUP; 2) The soil in the experimental station is characterized by high initial N contents ($\text{NO}_3\text{-N}$ and $\text{NH}_4\text{-N}$), which can, therefore, result in a daily concentration for passive root NUP higher than the C_{max} value considered in the simulation, thereby decreasing the effect of additional N inputs on NUP. In other words, the simulated NUP was derived from initial soil inorganic N contents and remained limited even though high N contents are available for wheat. Karandish and Šimůnek (2017) pointed out that to accurately simulate NUP, it is necessary to well calibrate and validate the C_{max} value. According to the simulation results, $\text{NO}_3\text{-N}$ was the main N form assimilated by wheat (>99%) due to the rapid nitrification of $\text{NH}_4\text{-N}$ and the consideration of passive NUP in the simulation. The NUP amount accounted for 5.1% of the total initial N, which is consistent with the results of Karandish and Šimůnek (2017) and Madathil et al. (2019).

The volatilized and denitrified amounts increased considerably with increasing N fertilizer rates. Nevertheless, the denitrification process was the main contributor to $\text{NO}_3\text{-N}$ loss at Douyet. At the control (N0), the volatilized and denitrified amounts accounted for 5.6 and 58% of initial soil N, respectively, which is consistent with the findings of Mokari et al. (2019) and Li et al. 2015, showing N denitrification as the predominant N loss pathway using HYDRUS-1D. The optimized first-rate constants showed that the denitrification pathway occurred within the 20–80 cm soil layer. The high denitrified amount might be due to the presence of high initial $\text{NH}_4\text{-N}$ and $\text{NO}_3\text{-N}$ contents of 269 and 534 kg ha^{-1} , respectively, and some physical characteristics of the soil, such as poor drainage and high-water retention capacity (Butterbach-Bahl and Dannenman, 2011). Nevertheless, the denitrified amount might be overestimated due to two main reasons: 1) The first-order constants of denitrification were optimized in this study to achieve minimal errors between the observed and simulated $\text{NO}_3\text{-N}$ concentrations. Therefore, the slight underestimations of the simulated $\text{NO}_3\text{-N}$ contents due to the insufficient data used for the calibration of HYDRUS-1D and negligence of other soil parameters that affect $\text{NO}_3\text{-N}$ transport are probably the main causes of this overestimation; 2) HYDRUS-1D software assumes that the denitrification pathway is a first-order reaction, taking into consideration $\text{NO}_3\text{-N}$ contents and SWC of the root zone (Eq. 1). Since the soil field is characterized by high initial N contents and fine soil texture, the denitrification pathway could, therefore, be substantially strengthened during the simulation. According to the simulation results, most soil $\text{NH}_4\text{-N}$ (about 92% of the total $\text{NH}_4\text{-N}$ content) was rapidly nitrified within a few days, which is consistent with the findings reported by Berlin et al. (2015), Eltarabily et al. (2019), Madathil et al. (2019), and Chen et al. (2020). Therefore, the high nitrification rate of $\text{NH}_4\text{-N}$ could increase the $\text{NO}_3\text{-N}$ contents in the soil profile and, consequently, enhance the denitrification pathway without necessarily requiring waterlogging conditions, which is consistent with the results of Johnson and

Raun (1995) and Forte and Fierro (2019). As mentioned above, N immobilization was ignored in the simulation, thus the denitrified amount might include the N immobilized amount. The same denitrification behavior was observed under N fertilizer scenarios (N1, N2, N3, N4, and N5), showing a substantial N loss through denitrification, which is consistent with the results of Tan et al. (2015). According to the simulated N balance, the applied $\text{NH}_4\text{-N}$ was almost totally nitrified (about 96%). Therefore, the increase in the $\text{NO}_3\text{-N}$ contents from the applied $\text{NO}_3\text{-N}$ fertilizer and nitrified $\text{NH}_4\text{-N}$ might enhance considerably the N loss pathways. The volatilization and denitrification amounts accounted for 3.8 and 51.7% of the applied N fertilizer, respectively. The remaining part of the fertilizer contributed to the increase in residual $\text{NO}_3\text{-N}$ in the soil profile. According to our results, the initial N content, soil texture, and rainfall amount affected NUP and $\text{NO}_3\text{-N}$ leaching from N fertilizer at Douyet in the Saiss basin.

4. Conclusions

In this study, HYDRUS-1D software was used to simulate soil water and $\text{NO}_3\text{-N}$ transport in a wheat field at Douyet in the Saiss basin under rainfed conditions and various N fertilization rates. By considering the 0–100 cm soil profile, we obtained minimal simulation errors between the measured and simulated SWC using the optimized hydraulic parameters through the inverse solution method of HYDRUS-1D at 42, 70, 96, 126, and 187 DAS. However, although HYDRUS-1D fairly accurately simulated the effects of N fertilizer rates on the $\text{NO}_3\text{-N}$ contents at the upper soil layer (0–20 cm), the simulated $\text{NO}_3\text{-N}$ contents were underestimated compared to the observed $\text{NO}_3\text{-N}$ contents, which might be due to the insufficient data used to calibrate HYDRUS-1D software and negligence of other factors affecting $\text{NO}_3\text{-N}$ transport (e.g., organic matter mineralization and N immobilization). The RMSE and MAE values of $\text{NO}_3\text{-N}$ transport simulation increased with increasing N fertilizer rates, more particularly at the 0–20 cm soil layer. In addition, the effects of N fertilizer rates on NUP and $\text{NO}_3\text{-N}$ leaching were negligible. The $\text{NO}_3\text{-N}$ leached amount was about 25 kg ha^{-1} in all N fertilizer scenarios, indicating that the leached $\text{NO}_3\text{-N}$ was derived from the initial N contents. $\text{NO}_3\text{-N}$ leaching occurred mainly in the initial wheat stage. Indeed, the insufficient rainfall amount recorded, fine soil texture, and low soil hydraulic conductivity affected negatively water percolation and $\text{NO}_3\text{-N}$ leaching. According to the simulated N balance, the volatilization and denitrification pathways were the main N-loss pathways of N fertilizer at Douyet. The volatilization and denitrification amounts accounted for 3.8 and 51.7% of the applied N fertilizer, respectively.

Although the optimized input parameters varied within the range reported in previous studies and were fairly suitable for simulating SWC and $\text{NO}_3\text{-N}$ in all N fertilizer scenarios, further long-term studies are required to calibrate HYDRUS-1D using sufficient data and to assess its simulation accuracy under several climatic conditions. In addition, further studies on the comparison of the simulation accuracy in one-, two-, and three-dimensional domains are also required.

Funding

The authors received no financial support for the research, authorship, and/or publication of this article.

Competing of interests

The authors have no relevant financial or non-financial interests to disclose.

References

- Allen, R.G., Pereira, L.S., Raes D., Smith, M., 1998. Crop evapotranspiration: Guidelines for computing crop water requirements. FAO Irrigation and Drainage, Rome.
- Azad, N., Behmanesh, J., Rezaverdinejad, V., Abbasi, F., Navabian, M., 2019. Evaluation of fertigation management impacts of surface drip irrigation on reducing nitrate leaching using numerical modeling. *Environmental Science and Pollution Research* 26, 36499-36514. <https://doi.org/10.1007/s11356-019-06699-2>
- Badr, M.A., El-Tohamy, W.A., Zaghoul, A.M., 2012. Yield and water use efficiency of potato grown under different irrigation and nitrogen levels in an arid region. *Agricultural Water Management* 110, 9–15. <https://doi.org/10.1016/j.agwat.2012.03.008>
- Baram, S., Couvreur, V., Harter, T., Read, M., Brown, P.H., Kandelous, M., Smart D.R., Hopmans, J.W., 2016. Estimating Nitrate Leaching to Groundwater from Orchards: Comparing Crop Nitrogen Excess, Deep Vadose Zone Data-Driven Estimates, and HYDRUS Modeling. *Vadose Zone Journal* 15(11), 1–13. <https://doi.org/10.2136/vzj2016.07.0061>
- Butterbach-Bahl, K., Dannenmann, M., 2011. Denitrification and associated soil N₂O emissions due to agricultural activities in a changing climate. *Current Opinion in Environmental Sustainability* 3(5), 389–395. <https://doi.org/10.1016/j.cosust.2011.08.004>
- Barraclough, P.B., 1986. The growth and activity of winter wheat roots in the field: nutrient inflows of high-yielding crops. *The Journal of Agricultural Science* 106(01), 53–59. <https://doi.org/10.1017/S0021859600061724>
- Bendidi, A., Daoui, K., Kajji, A., Dahan, R., Ibriz, M., 2013. Effects of Supplemental Irrigation and Nitrogen Applied on Yield and Yield Components of Bread Wheat at the Sads Region of Morocco. *American Journal of Experimental Agriculture* 3(4), 904–9013.
- Berlin, M., Nambi, I.M., Kumar, G.S., 2015. Experimental and numerical investigations on nitrogen species transport in unsaturated soil during various irrigation patterns. *Sadhana* 40(8), 2429–2455. <https://doi.org/10.1007/s12046-015-0420-4>
- Bourziza, R., Hammani, A., Mailhol, J.C., Bouaziz, A., Kuper, M., 2017. Modeling subsurface drip irrigation for date palm under oasis conditions, *Cahiers Agricultures* 26(3), 35007. <https://doi.org/10.1051/cagri/2017023>
- Chen, N., Li, X., Šimůnek, J., Shi, H., Hu, Q., Zhang, Y., 2020. Evaluating soil nitrate dynamics in an intercropping dripped ecosystem using HYDRUS-2D. *Science of the Total Environment* 718, 137314. <https://doi.org/10.1016/j.scitotenv.2020.137314>
- Chen, K., Yu, S., Ma, T., Ding, J., He, P., Li, Y., Dai, Y., Zeng, G., 2022. Modeling the Water and Nitrogen Management Practices in Paddy Fields with HYDRUS-1D. *Agriculture* 12, 924. <https://doi.org/10.3390/agriculture12070924>
- Dash, C.J., Sarangi, A., Singh, D.K., Singh, A.K., Adhikary, P.P., 2014. Prediction of root zone water and nitrogen balance in an irrigated rice field using a simulation model. *Paddy and Water Environment* 13(3), 281–290. <https://doi.org/10.1007/s10333-014-0439-x>
- Ebrahimian, H., Liaghat, A., Parsinejad, M., Abbasi, F., Navabian, M., (2012). Comparison of One- and Two-Dimensional Models to Simulate Alternate and Conventional Furrow Fertigation. *Journal of Irrigation and Drainage Engineering* 138(10), 929–938. [https://doi.org/10.1061/\(ASCE\)IR.1943-4774.0000482](https://doi.org/10.1061/(ASCE)IR.1943-4774.0000482)
- Eltarably, M.G., Burke, J.M., Bali, K.M., (2019). Effect of Deficit Irrigation on Nitrogen Uptake of Sunflower in the Low Desert Region of California. *Water* 11(11), 2340. <https://doi.org/10.3390/w11112340>
- Fang, Q., Yu, Q., Wang, E., Chen, Y., Zhang, G., Wang, J., Li, L., 2006. Soil nitrate accumulation, leaching and crop nitrogen use as influenced by fertilization and irrigation in an intensive wheat–maize double cropping system in the North China Plain. *Plant and Soil* 284(1–2), 335–350. <https://doi.org/10.1007/s11104-006-0055-7>
- Feddes, R.A., Kowalik, P.J., Zaradny, H., 1978. Simulation of field water use and crop yield. Simulation monographs Wageningen
- Fekkoul, A., Zarhloule, Y., Boughriba, M., Barkaoui, A., Jilali, A., Bouri, S., 2012. Impact of anthropogenic activities on the groundwater resources of the unconfined aquifer of Triffa plain (Eastern Morocco). *Arabian Journal of Geosciences* 6(12), 4917–4924. <https://doi.org/10.1007/s12517-012-0740-1>
- Forte, A., Fierro, A., 2019. Denitrification Rate and Its Potential to Predict Biogenic N₂O Field Emissions in a Mediterranean Maize-Cropped Soil in Southern Italy, *Land* 8(6), 97. <https://doi.org/10.3390/land8060097>
- Johnson, G.V., Raun, W.R., 1995. Nitrate leaching in continuous winter wheat: Use of a soil-plant buffering concept to account for fertilizer nitrogen, *Journal of Production Agriculture* 8(4), 486. <https://doi.org/10.2134/jpa1995.0486>
- Gelhar, L.W., Welty, C., Rehfeldt, K.R., 1992. A critical review of data on field scale dispersion in aquifers. *Water Resources Research* 28(7), 1955–1974.
- Hanson, B.R., Šimůnek, J., Hopmans, J.W., 2006. Evaluation of urea–ammonium–nitrate fertigation with drip irrigation using numerical modeling. *Agricultural Water Management* 86(1–2), 102–113. <https://doi.org/10.1016/j.agwat.2006.06.013>
- Iqbal, M., Kamal, M.R., Fazly, M.F., Che Man, H., Wayayok, A., 2019. HYDRUS-1D Simulation of Soil Water Dynamics for Sweet Corn under Tropical Rainfed Condition. *Applied Sciences* 10(4), 1219. <https://doi.org/10.3390/app10041219>
- Kadyampakeni, D.M., Morgan, K.T., Nkedi-Kizza, P., Schumann, A.W., Jawitz, J.W., 2018. Modeling Water and Nutrient Movement in Sandy Soils Using HYDRUS-2D. *Journal of Environmental Quality* 47(6), 1546–1553. <https://doi.org/10.2134/jeq2018.02.0056>
- Kandelous, M.M., Šimůnek, J., 2010. Numerical simulations of water movement in a subsurface drip irrigation system under field and laboratory conditions using HYDRUS-2D. *Agricultural Water Management* 97(7), 1070–1076. <https://doi.org/10.1016/j.agwat.2010.02.012>
- Karandish, F., Šimůnek, J., 2017. Two-dimensional modeling of nitrogen and water dynamics for various N-managed water-saving irrigation strategies using HYDRUS. *Agricultural Water Management* 193, 174–190. <https://doi.org/10.1016/j.agwat.2017.07.023>
- Lahjouj, A., El Hmadi, A., Bouhafa, K., 2020a. Spatial and statistical assessment of nitrate contamination in groundwater: Case of Sais basin, Morocco. *Journal of Groundwater Science and Engineering* 8(2), 147–157. <https://doi.org/10.19637/j.cnki.2305-7068.2020.02.006>
- Lahjouj, A., El Hmadi, A., Bouhafa, K., Boufala, M., 2020b. Mapping specific groundwater vulnerability to nitrate using random forest: case of Sais basin, Morocco. *Modeling Earth Systems and Environment* 6, 1451–1466. <https://doi.org/10.1007/s40808-020-00761-6>
- Li, Y., Šimůnek, J., Zhang, Z., Jing, L., Ni, L. 2015. Evaluation of nitrogen balance in a direct-seeded-rice field experiment using Hydrus-1D. *Agricultural Water Management* 148, 213–222. <https://doi:10.1016/j.agwat.2014.10.010>
- Liao, L., Zhang, L., Bengtsson, L. 2008. Soil moisture variation and water consumption of spring wheat and their effects on crop yield under

- drip irrigation. *Irrigation and Drainage Systems* 22(3–4), 253–270. <https://doi.org/10.1007/s10795-008-9055-5>
- Ling, G., El-Kadi, A.I., 1998. A lumped parameter model for nitrogen transformation in the unsaturated zone. *Water Resources Research* 34(2), 203–212. <https://doi.org/10.1029/97WR02683>
- Liu, X., Ju, X., Zhang, F., Pan, J., Christie, P., 2003. Nitrogen dynamics and budgets in a winter wheat–maize cropping system in the North China Plain. *Field Crops Research* 83(2), 111–124. [https://doi.org/10.1016/S0378-4290\(03\)00068-6](https://doi.org/10.1016/S0378-4290(03)00068-6)
- Madathil, M.S.P., Aggarwal, P., Krishnan, P., Rai, V., Pramanik, P., Das, T.K., 2019. Modeling the temporal distribution of water, ammonium-N, and nitrate-N in the root zone of wheat using HYDRUS-2D under conservation agriculture. *Environmental Science and Pollution Research* 27, 2197–2216. <https://doi.org/10.1007/s11356-019-06642-5>
- Malhi, S.S., Johnston, A.M., Schoenau, J.J., Wang, Z.H., Vera, C.L., 2006. Seasonal biomass accumulation and nutrient uptake of wheat, barley and oat on a Black Chernozem soil in Saskatchewan. *Canadian Journal of Plant Science* 86, 1005–1014. <https://doi.org/10.4141/P05-116>
- Marinov, I., Marinov, A.M., 2014. A Coupled Mathematical Model to Predict the Influence of Nitrogen Fertilization on Crop, Soil and Groundwater Quality. *Water Resources Management* 28(15), 5231–5246. <https://doi.org/10.1007/s11269-014-0664-5>
- Marquardt, D.W., 1963. An Algorithm for Least-Squares Estimation of Nonlinear Parameters. *Journal of the Society for Industrial Applied Mathematics* 11(2), 431–441.
- Masetti, M., Poli, S., Sterlacchini, S., 2007. The Use of the Weights-of-Evidence Modeling Technique to Estimate the vulnerability of groundwater to nitrate contamination. *Natural Resources Research* 16(2), 109–119. <https://doi.org/10.1007/s11053-007-9045-6>
- Ministry of Agriculture, Fisheries, Rural Development and Water and Forestry (MAFRDWF), (2019) *StatAgri*.
- Mokari, E., Shukla, M.K., Šimůnek, J., Fernandez, J.L., 2019. Numerical Modeling of Nitrate in a Flood-Irrigated Pecan Orchard. *Soil Science Society of America Journal* 83(3), 555–564. <https://doi.org/10.2136/sssaj2018.11.0442>
- Mualem, Y., 1976. A new model for predicting the hydraulic conductivity of unsaturated porous media. *Water Resources Research* 12(3), 513–522.
- Narjary, B., Kumar, S., Meena, M.D., Kamra, S.K., & Sharma, D.K., 2020. Effects of Shallow Saline Groundwater Table Depth and Evaporative Flux on Soil Salinity Dynamics using Hydrus-1D. *Agricultural Research* 10, 105–115. <https://doi.org/10.1007/s40003-020-00484-1>
- Ogrinc, N., Tamšič, S., Zavadlav, S., Vrzel, J., Jin, L., 2019. Evaluation of geochemical processes and nitrate pollution sources at the Ljubljansko polje aquifer (Slovenia): A stable isotope perspective. *Science of the Total Environment* 646, 1588–1600. <https://doi.org/10.1016/j.scitotenv.2018.07.245>
- Pang, X.P., Gupta, S.C., Moncrief, J.F., Rosen, C.J., Cheng, H.H., 1998. Evaluation of Nitrate Leaching Potential in Minnesota Glacial Outwash Soils using the CERES-Maize Model. *Journal of Environmental Quality* 27(1), 75–85. <https://doi.org/10.2134/jeq1998.00472425002700010012x>
- Petersen, J., 2001. Recovery of 15N-ammonium- 15N-nitrate in spring wheat as affected by placement geometry of the fertilizer band. *Nutrient Cycling in Agroecosystems* 61(3), 215–221. <https://doi.org/10.1023/A:1013756715438>
- Phogat, V., Skewes, M.A., Cox, J.W., Sanderson, G., Alam, J., Šimůnek, J., 2014. Seasonal simulation of water, salinity and nitrate dynamics under drip irrigated mandarin (*Citrus reticulata*) and assessing management options for drainage and nitrate leaching. *Journal of Hydrology* 513, 504–516. <https://doi.org/10.1016/j.jhydrol.2014.04.008>
- Ramos, T.B., Šimůnek, J., Gonçalves, M.C., Martins, J.C., Prazeres, A., Pereira, L.S. 2012. Two-dimensional modeling of water and nitrogen fate from sweet sorghum irrigated with fresh and blended saline waters. *Agricultural Water Management* 111, 87–104. <https://doi.org/10.1016/j.agwat.2012.05.007>
- Rezayati, S., Khaledian, M., Razavipour, T., Rezaei, M., 2020. Water flow and nitrate transfer simulations in rice cultivation under different irrigation and nitrogen fertilizer application managements by HYDRUS-2D model. *Irrigation Science* 38, 353–363. <https://doi.org/10.1007/s00271-020-00676-1>
- Serio, F., Miglietta, P.P., Lamastra, L., Ficocelli, Intini, F., De Leo, F., De Donno, A., 2018. Groundwater nitrate contamination and agricultural land use: A grey water footprint perspective in Southern Apulia Region (Italy). *Science of the Total Environment* 645, 1425–1431. <https://doi.org/10.1016/j.scitotenv.2018.07.241>
- Shapiro, S.S., Wilk, M.B., 1965. An Analysis of Variance Test for Normality (Complete Samples). *Biometrika* 52(3–4), 591–611.
- Šimůnek, J., Van Genuchten, M.T., Šejna, M., 2008. Development and Applications of the HYDRUS and STANMOD Software Packages and Related Codes. *Vadose Zone Journal* 7(2), 587–600. <https://doi.org/10.2136/vzj2007.0077>
- Tan, X., Shao, D., Gu, W., Liu, H., 2015. Field analysis of water and nitrogen fate in lowland paddy fields under different water managements using HYDRUS-1D. *Agricultural Water Management* 150, 67–80. <https://doi.org/10.1016/j.agwat.2014.12.005>
- Wallace, A.J., Armstrong, R.D., Grace, P.R., Scheer, C., Partington, B.L., 2020. Nitrogen use efficiency of 15N urea applied to wheat based on fertiliser timing and use of inhibitors. *Nutrient Cycling in Agroecosystems* 116, 41–56. <https://doi.org/10.1007/s10705-019-10028-x>
- Wallis, K.J., Candela, L., Mateos, R.M., Tamoh, K., 2011. Simulation of nitrate leaching under potato crops in a Mediterranean area. Influence of frost prevention irrigation on nitrogen transport. *Agricultural Water Management* 98(10), 1629–1640. <https://doi.org/10.1016/j.agwat.2011.06.001>
- Wang, Q., Li, F., Zhao, L., Zhang, E., Shi, S., Zhao, W., Song, W., Vance, M.M., 2010. Effects of irrigation and nitrogen application rates on nitrate nitrogen distribution and fertilizer nitrogen loss, wheat yield and nitrogen uptake on a recently reclaimed sandy farmland. *Plant and Soil* 337(1–2), 325–339. <https://doi.org/10.1007/s11104-010-0530-z>
- Wang, Z., Li, J., Li, Y., 2014. Simulation of nitrate leaching under varying drip system uniformities and precipitation patterns during the growing season of maize in the North China Plain. *Agricultural Water Management* 142, 19–28. <https://doi.org/10.1016/j.agwat.2014.04.013>
- Wesseling, J.G., Elbers, J.A., Kabat, P., van den Broek, B.J., 1991. *SWATRE: instructions for input*, Internal Note, Winand Staring Centre, Wageningen, The Netherlands
- Willmott, C.J., 1982. Some comments on the evaluation of model performance. *Bulletin of the American Meteorological Society* 63(11), 1309–1313.
- Yang, S., Wang, Y., Liu, R., Xing, L., Yang, Z., 2018. Improved crop yield and reduced nitrate nitrogen leaching with straw return in a rice-wheat rotation of Ningxia irrigation district. *Scientific Report* 8, 9458. <https://doi.org/10.1038/s41598-018-27776-5>
- Zhang, X., Wang, Q., Xu, J., Gilliam, F.S., Tremblay, N., Li, C., 2015. In Situ Nitrogen Mineralization, Nitrification, and Ammonia Volatilization in Maize Field Fertilized with Urea in Huanghuaihai Region of Northern China. *PLoS one* 10(1). <https://doi.org/10.1371/journal.pone.0115649>
- Zhou, J., Cheng, G., Li, X., Hu, B.X., & Wang, G., 2012. Numerical Modeling of Wheat Irrigation using Coupled HYDRUS and WOFOST Models. *Soil Science Society of America Journal* 76(2), 648. <https://doi.org/10.2136/sssaj2010.0467>
- Zotarelli, L., Dukes, M.D., Scholberg, J.M.S., Muñoz-Carpena, R., Icerman, J., 2009. Tomato nitrogen accumulation and fertilizer use efficiency on a sandy soil, as affected by nitrogen rate and irrigation scheduling. *Agricultural Water Management* 96(8), 1247–1258. <https://doi.org/10.1016/j.agwat.2009.03.019>